ANL-HEP-TR-00-24

GAP2000-001

CONTINUED STUDY OF THE TIME STABILITY OF A SMALL WATER CERENKOV DETECTOR

D. Strom,[a,c] H. Glass,[a] H. Spinka,[b] and M. Thomure[a]

[a] Fermi National Accelerator Laboratory, Batavia, IL 60510
[b] Argonne National Laboratory, Argonne, IL 60439
[c] Augustana College, Rock Island, IL 61201

24 November, 1999

This note describes continued studies at Fermilab of the long term stability of a small water Cerenkov tank. Previous results are presented in Refs. [1,2] for studies between November, 1997 and October, 1998. The data given here continue these measurements through December, 1998, when the tank and electronics were moved to a different location, and then to November, 1999.

The water tank, bag liner, water, photomultiplier tube, and data acquisition software were unchanged for the additional measurements from June to November, 1999. However, some details of the geometry of the trigger counters relative to the tank and of the electronics may have differed. The setup for the 1999 results is described in this note.

The same analog-to-digital converter (ADC) was used for both time periods. Its pedestal was quite stable during the 1997-1998 measurements, but sizeable changes were observed in the more recent runs. As a result, dedicated pedestal runs were performed, and a number of additional tests were conducted.

EXPERIMENTAL LAYOUT

A schematic of the experimental setup is shown in Fig. 1. A pair of scintillation counters above and a second pair of scintillators below the tank were used to initiate the readout of the integrated signal from the photomultiplier in the water Cerenkov tank. The goal was to use cosmic ray muons that triggered all four scintillators and that passed approximately vertically through the water in the tank. These muons also passed through lead surrounding the lower pair of counters, so that their energy loss was approximately minimum ionizing. The path of the cosmic ray muons was chosen to be offset from the center of the tank so that most of them would not pass through the photomultiplier, where they might produce Cerenkov light in the glass face of the tube.

Work supported in part by the U.S. Department of Energy, Division of High Energy Physics, Contract W-31-109-ENG-38.

DISCLAIMER

Portions of this document may be illegible in electronic image products. Images are produced from the best available original document.

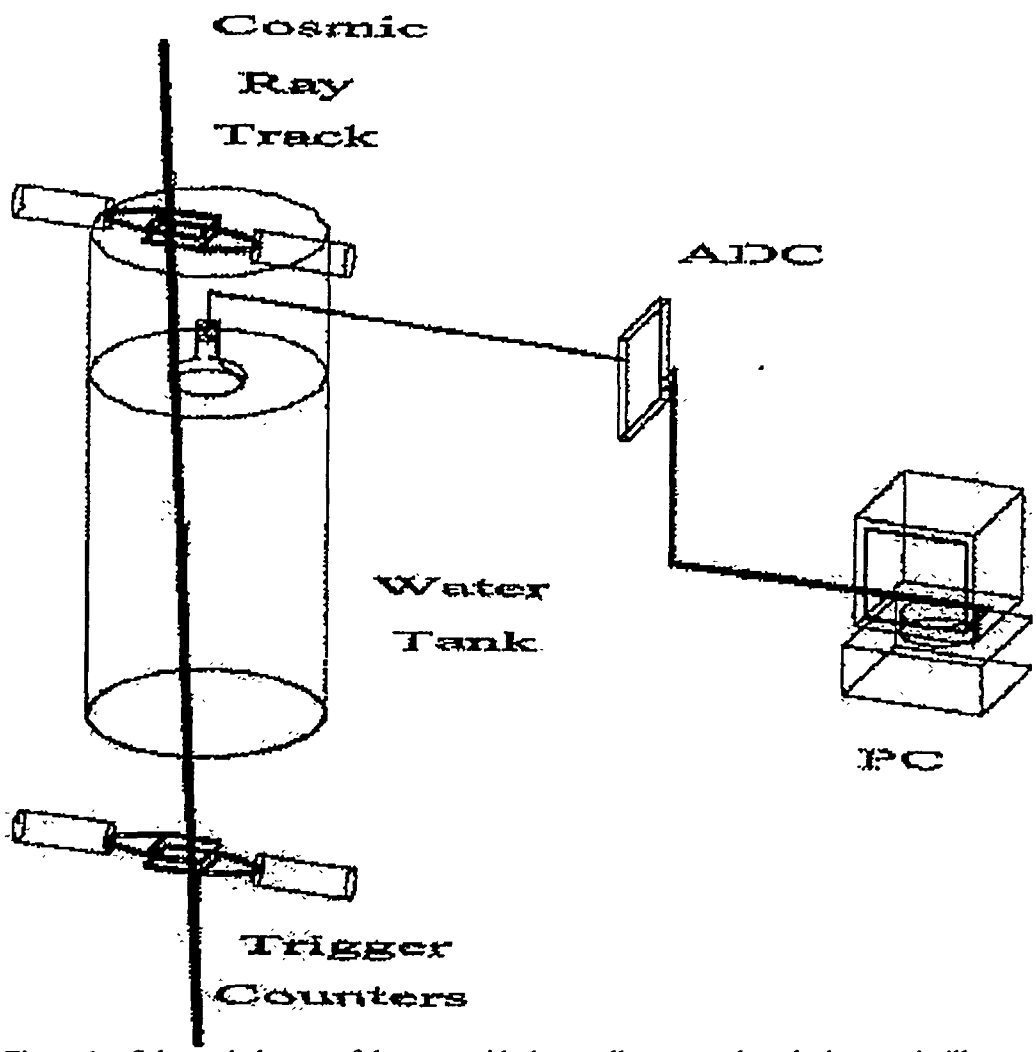

Figure 1. Schematic layout of the tests with the small water tank and trigger scintillators.

The tank, liner, water, and photomultiplier were moved together over a distance of several km in February, 1999. Except for any unintended consequences of the move, no other changes were made to this detector. Thus the 8" photomultiplier (Hamamatsu R1408) and its resistive base were identical to the ones described in Refs. [1,2]. Similarly, the bag liner of polyethylene and Tyvek whose seams were thermally bonded, the 55 gallon steel drum/tank, and the water were not changed. The glass face of the photomultiplier was in contact with the water in a design similar to one from the large IMB proton decay experiment.

The trigger counters and cables may have differed from the earlier measurements, but such changes are expected to have quite minor impact on the types of triggered particles. Three of the four scintillators were 6" x 6" x ? " or 15.24 x 15.24 x 0.95 cm^3 in size, and the fourth one was 8" x 8" x ½" or 20.32 x 20.32 x 0.64 cm^3. All were viewed by single 2" photomultipliers through trapezoidal-shaped lucite light guides. These light guides pointed in opposite directions within each pair of trigger counters, as shown in Fig. 1.

Three counters were of identical construction to those used in the 1997-1998 experiments; some may actually have come from these earlier measurements.

The precise geometry for the 1999 runs is shown in Fig. 2 and probably changed somewhat from the 1997-1998 experiments. The lower pair of trigger scintillators were surrounded on two sides by 4" (10 cm), and on the top by 2" (5 cm) of lead bricks. This was done to "harden" the spectrum of cosmic ray muons detected. The lead extended about 3" (7.6 cm) beyond the active area of the trigger counters, both towards and away from the photomultiplier tube.

The high voltages of the four trigger counters were set by performing "plateau curves," or recording coincidence rates in the upper or lower pair of counters as a function of the high voltage for one counter of the pair. However, these did not quite have the classical shape of plateau curves typically obtained with accelerator beams. It is not known whether plateau curves were also performed for the four trigger counters used during 1997-1998 runs, or whether the high voltages of any counters in common were the same. However, records of data collection indicate that the high voltage power supply for the trigger counters was changed in the middle of 1998 because of hardware problems. Voltage to all photomultipliers was found off in November, 1998 (near day 230) probably due to an interruption in the Fermilab AC power. During the 1999 runs, the voltages on the photomultipliers were checked several times with a voltage divider and DVM. No changes were observed from June to November, 1999.

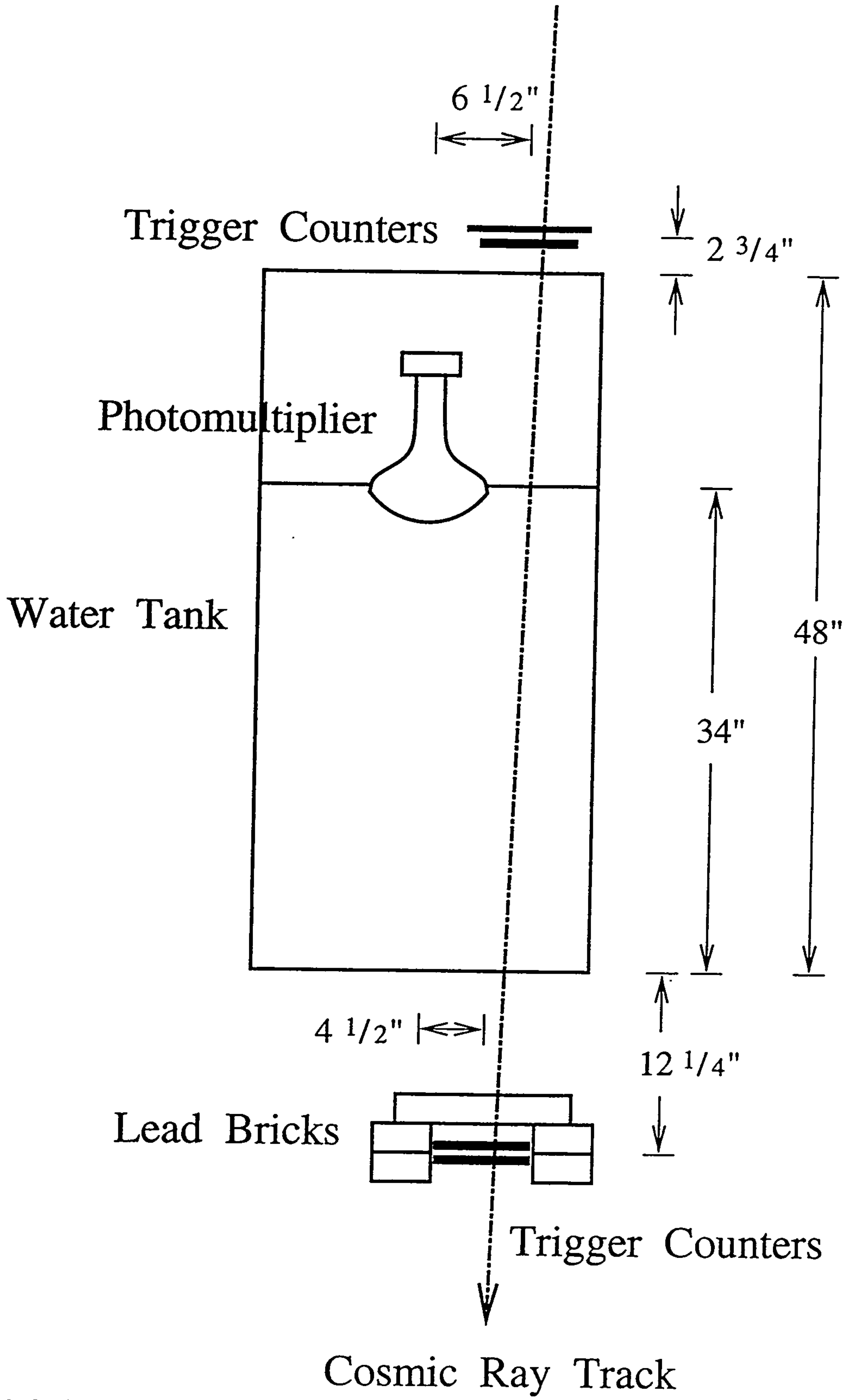

Figure 2. Scale drawing of the water Cerenkov tank, photomultiplier tube, trigger counters, and lead bricks for the 1999 runs.

ELECTRONICS AND DATA ACQUISITION

A schematic of the electronics is shown in Fig. 3. Most of the electronics modules and their settings were unchanged between the two run periods, though different cables were used in some cases. Similarly, the data acquisition software was unchanged.

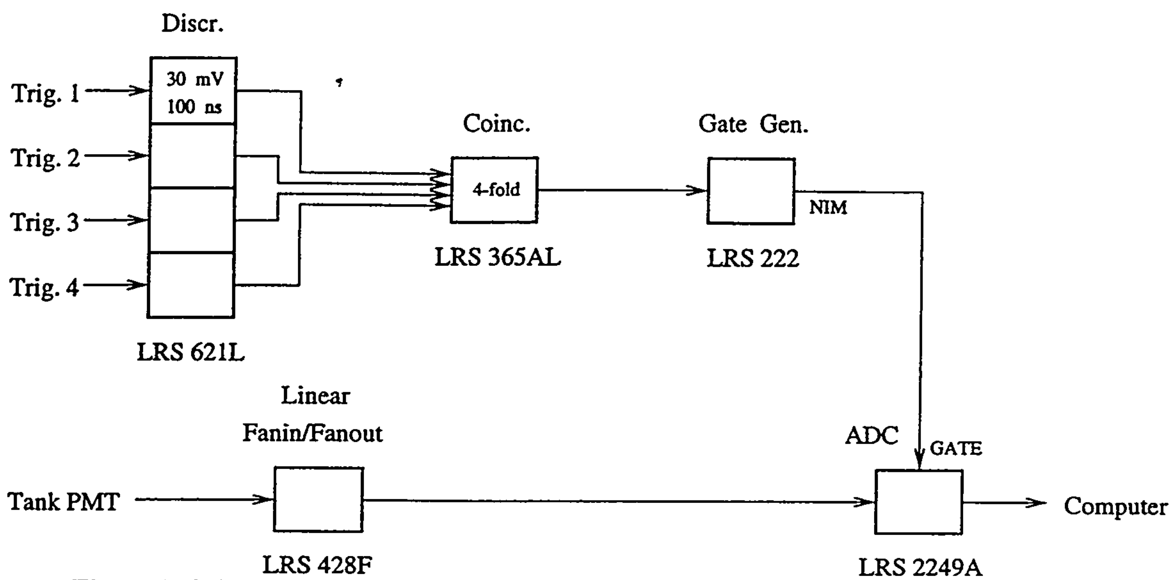

Figure 3. Schematic of the electronics for the small tank tests. All four channels of the discriminator had approximately the same threshold and width. The gate generator scale was 1 μsec, and the output width was adjusted to be about 250 nsec.

Negative high voltage for the trigger counters was supplied from a Fluke model 415B high voltage power supply and a Zener diode divider (homebuilt, type 11X 2562, from a LBL design). The positive high voltage for the photomultiplier inside the tank was also supplied from these same types of power supply and divider, and it was operated at a nominal voltage of +1060 V.

The signals from the trigger counter photomultipliers went to four channels of a LeCroy (LRS) model 621L NIM discriminator module, set to thresholds of 30 mV and output widths of 100 - 110 nsec. The outputs were required to form a 4-fold coincidence in a LRS 365AL module. The 50 nsec wide coincidence signal was sent to a LRS 222 gate generator module that supplied the 250 nsec gate to the ADC for the photomultiplier in the water tank. Typical 4-fold coincidence rates were 0.55 and 0.83 per minute during the 1997-1998 and the 1999 runs, respectively. The similarity of these rates suggests that the trigger selected a similar part of the steeply-falling cosmic ray energy spectrum.

The analog signal from the photomultiplier inside the water tank first went to a LRS 428F linear fan-in/fan-out and then to a LRS 2249A Camac ADC after appropriate cable delay. The ADC was read out via a LRS 8901A GPIB interface module to a Dell model 310 personal computer running Windows 3.1. The data acquisition software (light2.c) is a C program that interfaces with the electronics using calls to the National Instruments GPIB library. The program sets up the ADC to generate a Look-At-Me (LAM) whenever it receives a trigger, and the 8901A to generate a service request (SRQ) when it sees a

LAM. The program repeatedly polls the 8901A until it sees an SRQ. It then reads out the raw ADC values and re-arms the electronics for the next trigger. The ADC value was converted to integrated current using the nominal value of 0.25 picoCoulombs (pC) per channel for the ADC, and a fixed pedestal subtracted before the result was stored in an ascii file. The time of the event from the internal computer clock was also recorded in the file.

A typical spectrum from a 92 hr run in July 1999 is shown in Fig. 4 in both a linear and semi-logarithmic scale. The small peak near 30 pC corresponds to the pedestal value. This was confirmed by the results of dedicated pedestal runs taken close in time to the cosmic ray data using an ADC gate that occurred at a random time. The pedestal events are present in the cosmic ray data due to accidental coincidences. For example, two cosmic ray muons could occur close in time – one hitting the upper pair and the other striking the lower pair of trigger counters, but neither passing through the water tank. The rate of pedestal events in a normal cosmic ray run is roughly 0.6 per hour. Finally, the ADC saturated near 260 pC, leading to the excess of events observed in Fig. 4.

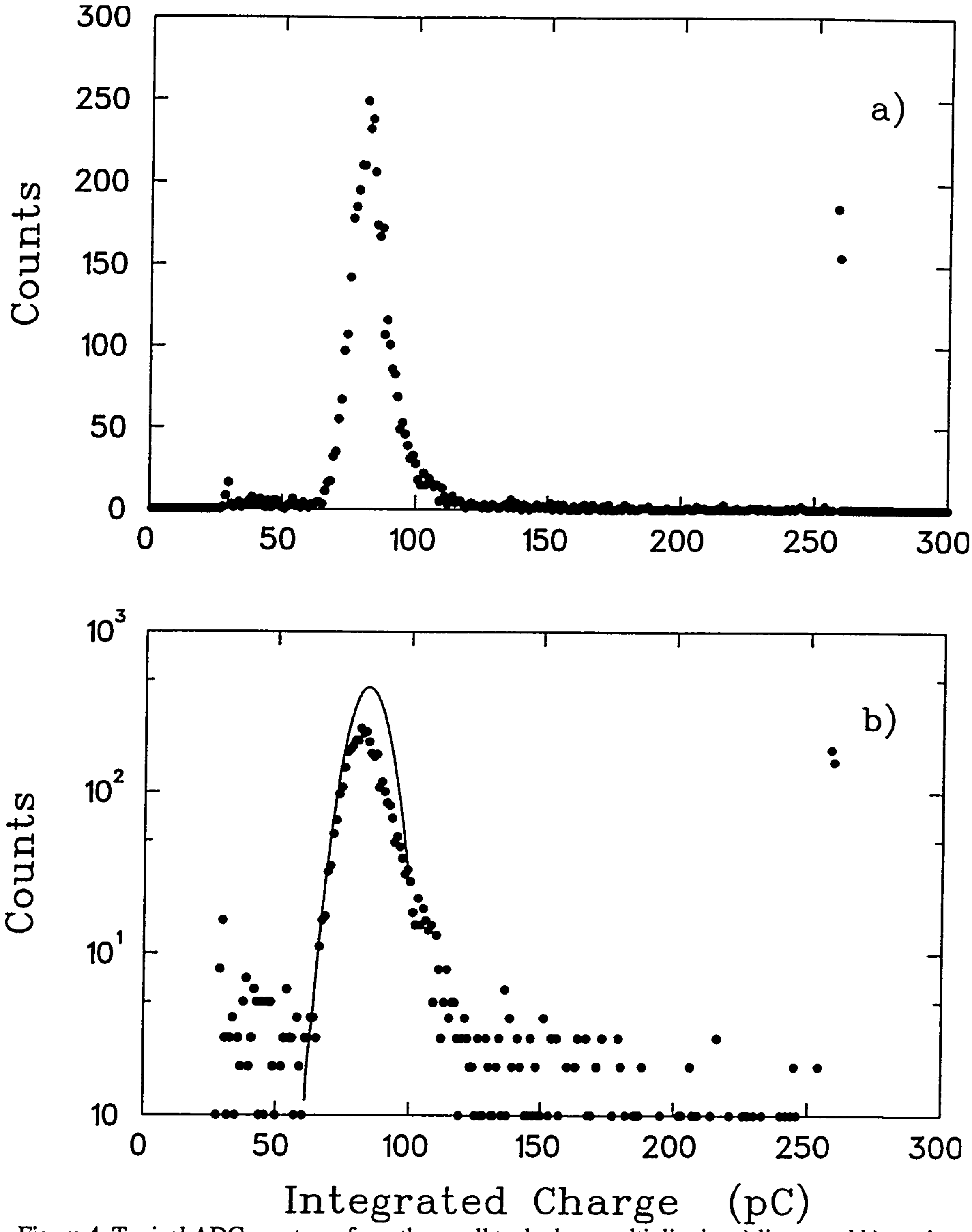

Figure 4. Typical ADC spectrum from the small tank photomultiplier in a) linear and b) semi-logarithmic scales. The pedestal is near 30 pC, saturation occurs near 260 pC, and the run number was tst2019. Results of a Gaussian fit to the peak from the EXCEL program is also shown; for most runs the fit is better than the one shown here.

DATA ANALYSIS

The raw data were analyzed in two ways; one using commercial software (Microsoft EXCEL), and the other using code written by one of the authors. The results from the two methods are quite similar, and differences allow estimates of systematic errors. They also permit checks on estimated statistical errors from the commercial software.

For the first type of analysis, the raw data were copied onto a computer cluster at Fermilab. The files were then read by the EXCEL spreadsheet software, and sorted into a histogram with bin width 2 pC using a macro. The pedestal was estimated as described below, and a Gaussian was fit to the events near the peak in the spectrum (about 80 pC in Fig. 4). A second macro was written to perform some of these calculations; details are included in Ref. [3].

The pedestal for both cosmic ray and pedestal runs was estimated in the same way. The mean ($\langle x \rangle_P$) and standard deviation (σ_P) were computed for all events in the pedestal region. This region was chosen to be 10 pC wide beginning with the lowest charge recorded in an event near the pedestal. For example, for the run in Fig. 4 (tst2019), the pedestal region included events between 28 and 38 pC, and the calculations gave $\langle x \rangle_P =$ 32.2 pC and $\sigma_P = 2.8$ pC. The uncertainty on the pedestal mean was

$$\sigma_{\langle x \rangle} = \sigma_P / (n - 1)^{1/2},$$

where n is the total number of events in the pedestal region. Table 1 contains a list of the pedestals and uncertainties, dates, and run numbers for all "useful runs" between March 1998 and December 1999, including dedicated pedestal runs; data from before March, 1998 were not available. Figure 5 gives a plot of the pedestal values as a function of time during the 1999 runs; the pedestal seemed to be close to zero and nearly constant during the 1998 runs analyzed. Considerable variation is observed in the 1999 pedestal values.

The fit to the peak in the cosmic ray spectrum was performed with EXCEL software as well. For most runs, the region in the spectrum from 60 – 100 pC, approximately centered on the peak, was fit with a Gaussian in order to estimate the peak position ($\langle x \rangle$) and width (σ). (For runs where the peak occurred at a value considerably different from 80 pC, other limits were used.) The fits were not very good, since the spectrum shape is clearly asymmetric and non-Gaussian, as can be seen in Fig. 4. The results are given in Table 2, along with an estimated error in $\langle x \rangle$. This uncertainty was taken to be

$$\delta(\langle x \rangle) \sim \sigma / N^{1/2},$$

where N is the total number of events from the Gaussian fit. The raw peak positions, $\langle x \rangle$, are plotted as a function of time during the 1999 runs in Fig. 6. The peaks corrected for the pedestals ($\langle y \rangle = \langle x \rangle - \langle x \rangle_P$) are given in Fig. 7. The raw peak positions show considerably larger variations than the values corrected for pedestals.

The number of photoelectrons corresponding to the peak in the ADC spectrum was computed from the relation

$$\#\,\text{p.e.} = 1.5 / (\sigma / \langle y \rangle)^2 ,$$

taken from Ref. [4]. Assuming negligible errors on the pedestal determination, the uncertainty in this estimate is

$$\delta\,(\#\,\text{p.e.}) = (\#\,\text{p.e.})\ (2 / N^{1/2})\ [N/(N-1) + \sigma^2 / \langle y \rangle^2]^{1/2} ,$$

which has the expected dependence on $N^{-1/2}$, for N the total number of events in the ADC spectrum peak. In addition, the effect of the pedestal uncertainty can be added in quadrature with the error estimate on the number of photoelectrons above, though this contribution was found to be small. The results for the number of photoelectrons are given in Fig. 8 with uncertainties shown for the case with the pedestal error included.

The alternate method for determining the peak and width of the ADC spectrum involved an iterative procedure. In the first step, the mean ($\langle x_1 \rangle$) of the events with integrated charge between 60 and 100 pC was computed. (Again, different limits were used when the peak occurred far from 80 pC.) For the second step, events in the range

$$\langle x_1 \rangle - 0.4\,(\langle x_1 \rangle - \langle x \rangle_P) < \text{Charge} < \langle x_1 \rangle + 0.4\,(\langle x_1 \rangle - \langle x \rangle_P)$$

were used to compute the mean, $\langle x_2 \rangle$, and the standard deviation, σ_2. For the third step, $\langle x_2 \rangle$ replaced $\langle x_1 \rangle$ in the limits above, and the calculations yielded $\langle x_3 \rangle$ and σ_3. This procedure was continued until the results converged. Such an iteration partially compensated for variation in the gain of the system. It would work best if the shape of the spectrum was unchanged except for the overall gain. The mean and standard deviation of the peak when the iteration converged are also given in Table 2 for a sampling of runs. Generally, the peak position was 1-2 pC less and the width was somewhat larger than the Gaussian fit using the EXCEL software. In addition, the number of events was usually slightly larger, mostly from the events on the high pulse height tail of the peak distribution.

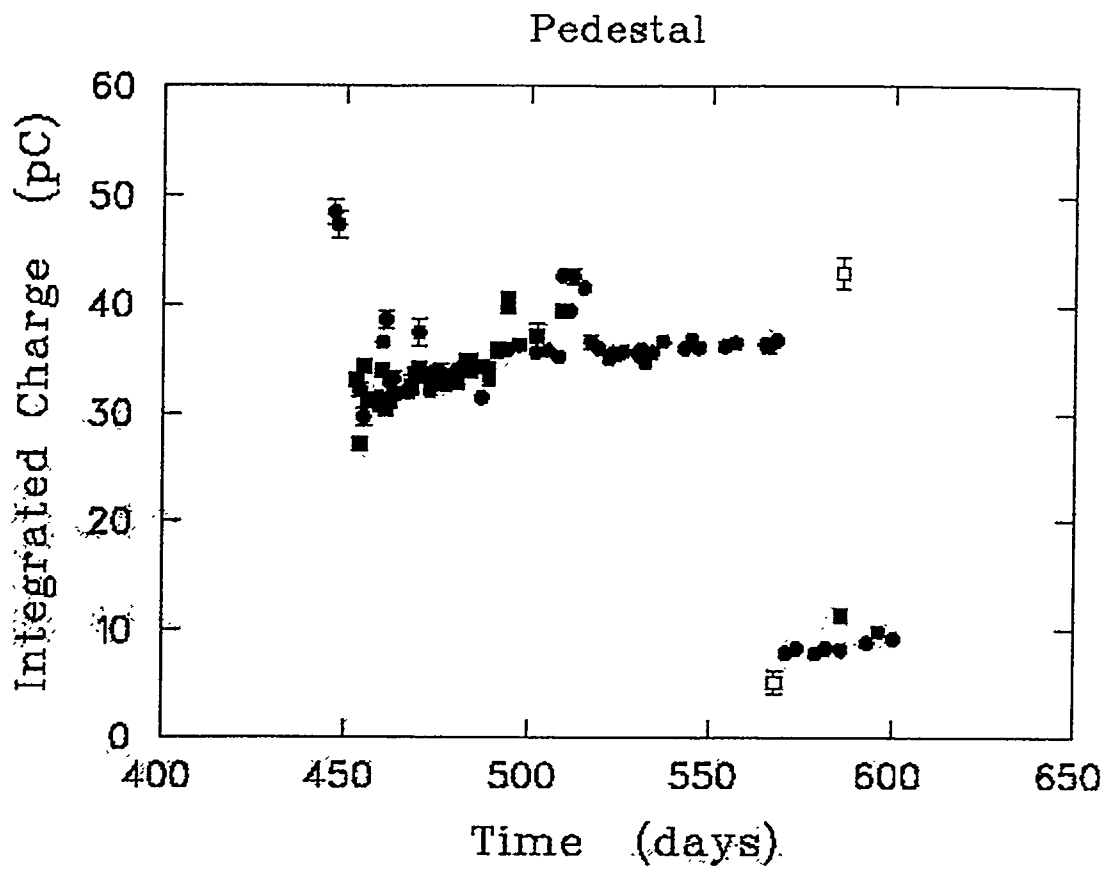

Figure 5. Variation of the pedestal in the ADC spectra as a function of time for the 1999 runs. The two runs denoted by open squares are test runs, as noted in the text. The solid squares are from dedicated pedestal runs and the solid circles from normal cosmic ray runs.

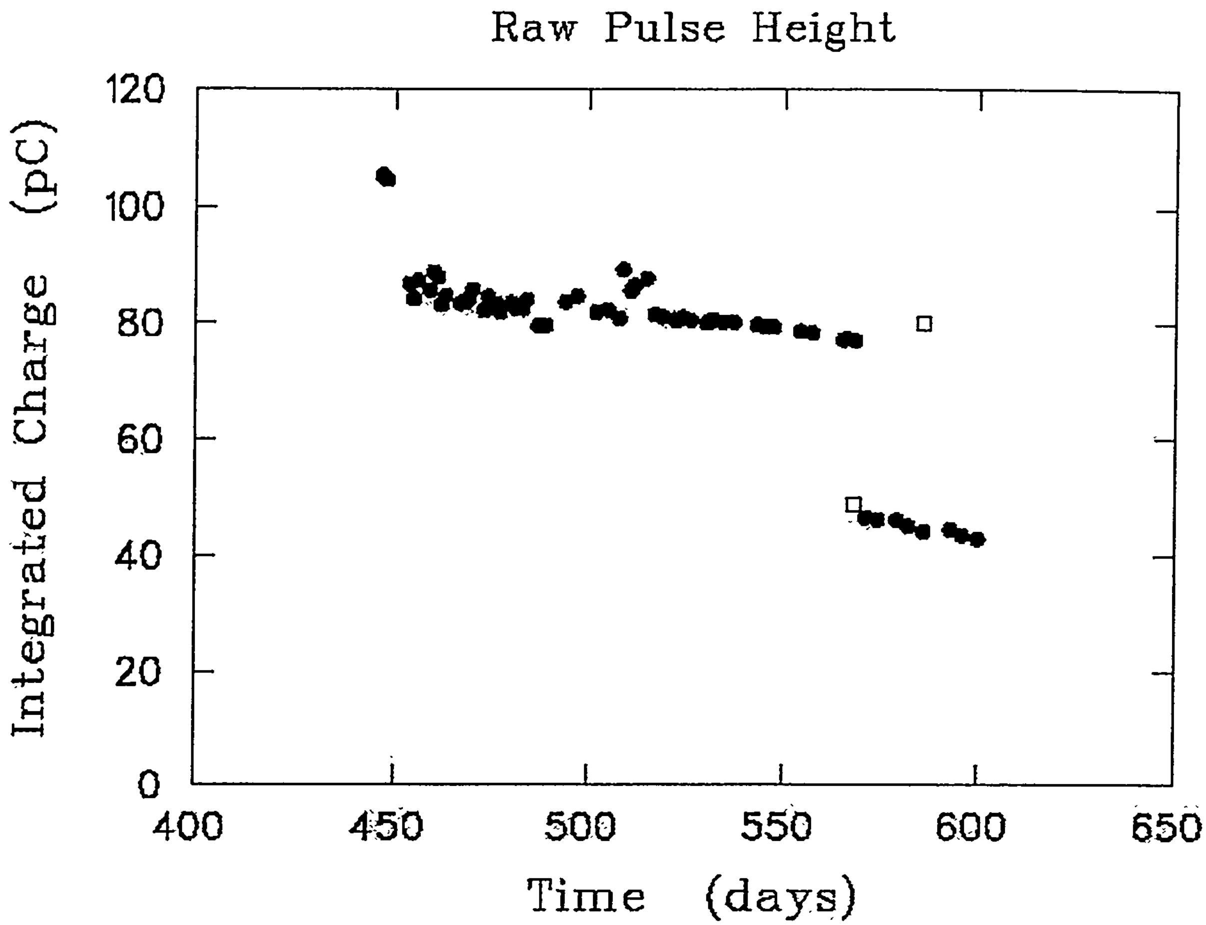

Figure 6. Plot of the raw peaks in the ADC spectra as a function of time for the 1999 runs. The peak positions were estimated from the Gaussian fits using EXCEL software. The computed uncertainties are smaller than the points. The results denoted by open squares are from test runs, as noted in the text.

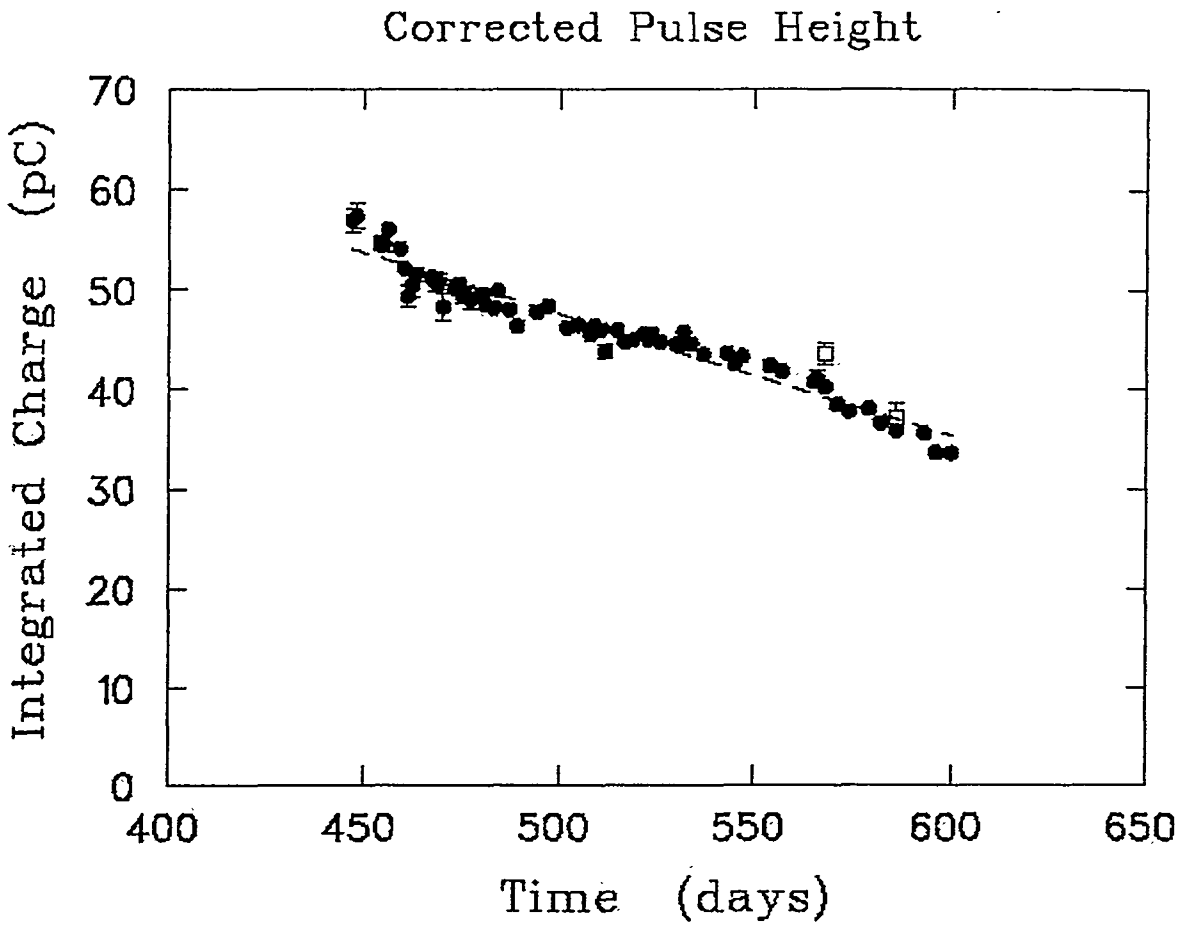

Figure 7. Plot of the peak positions in the ADC spectra, corrected by the pedestal values, as a function of time for the 1999 runs. The computed uncertainties are generally smaller than the points. The results denoted by open squares are from test runs, as noted in the text. The dashed curve is the straight line fit to the points.

RESULTS

Considerable variation is observed in the pedestal values with time shown in Figs. 5 and 9. Several discontinuities are apparent. The one in October, 1999 near day 570 occurred at the time of a test, as described below. There was also a jump in the pedestal at some time during early 1999, when no data were being collected and the move of the apparatus to the new location took place. Other discontinuities did not correspond to any hardware change. A gradual increase in the pedestal values with time until the sharp drop near day 570 is also apparent. In any case, such variation was not observed during the 1997 – 1998 measurements, before the move. It was also observed that the pedestal run and the cosmic ray run pedestals are generally in good agreement (these runs are mixed together in Figs. 5 and 9).

Similarly, Fig. 6 with the raw peak values shows considerable variations, also with discontinuities at the same times as the pedestal results. A gradual decrease in these peak values is also observed until the sharp drop near day 570.

By contrast, the peaks corrected for pedestals exhibit a smooth, decreasing behavior with time as can be seen in Fig. 7. On this basis, it is expected that the pedestal determination and subtraction have been done correctly and are necessary for these data. This decrease is consistent with neither linear nor exponential behavior. For example, a straight line fit to these data (shown in Fig. 7) gives

$$\text{Charge} = (-0.1220 \pm 0.0013) * \text{Time (days)} + (108.61 \pm 0.67),$$

with a $?^2$ / d.f. = 463.2 / 59 = 7.85 . The average drop from 16 June, 1999 (day 447) to 16 November, 1999 corresponds to approximately 80% / year if the peak values were to continue to fall linearly.

Two short test runs were conducted (tst2094 on day 568 and tst2101 on day 586) to check for problems with the electronics. In the first one, the LRS 2249A ADC was physically replaced with another, identical ADC. The original ADC was then put back for run tst2095 and all following data. A significant change in the pedestal occurred (Fig. 5), but the peak corrected for pedestal was close to that for other nearby runs (Fig. 7). However, the pedestal also changed for the original ADC when it was put back into the CAMAC crate!

The second test had a change in the channel of the LRS 428F linear fan-out. Again the pedestal changed but the peak corrected for pedestal did not. It was concluded from these two tests and the HV measurements that the drop in pulse height from the photomultiplier in the small tank was not due to electronics problems (photomultiplier HV, linear fan-out, or ADC). Furthermore, the tank is located inside a large building. The temperature was occasionally monitored from June to November, 1999 and varied from 73 to 76 °F, but not correlated with the season. This small temperature variation is not expected to be the cause of the sizeable drop in integrated charge either.

One further test was performed. If the gain of the R1408 photomultiplier was constant, but the amount of light reaching the tube was decreasing, then it would be expected that the calculated number of photoelectrons and the integrated charge would decrease together. In particular, the straight line fit from Fig. 7 should be roughly proportional to the number of photoelectrons. The scaled straight line fit is shown in Fig. 8 with a scale factor of (2.0 photoelectrons / pC). There is reasonable agreement with this line, but not with a constant value. This test reinforces the case for a drop in the amount of light reaching the photomultiplier.

On 16 November, 1999 it was decided to look into the small tank. No standing water was observed on top of the bag, and the photomultiplier base did not appear corroded. The water appeared clear and the photomultiplier glass had no obvious deposits present. The inside of the tyvek bag did not feel "slimy", and exhibited no apparent discoloration.

Unfortunately, the water was contaminated during the removal of the photomultiplier, so that the test with this small tank had to be concluded. (A chemical analysis of the water would have been meaningless.)

ACKNOWLEDGEMENTS

We wish to thank our Fermilab colleagues – Paul Mantsch, Peter Mazur, Carlos Hojvat, Lou Voyvodic, Rich Andrews, and Larry Coulson, and visitors Andrej Filipcic and Bai Xinhua – for their assistance with these studies. This work was supported in part by Fermilab, under contract with the U.S. Department of Energy, Division of High Energy Physics, and by an Argonne National Laboratory – University of Chicago collaborative grant. Authors Derek Stron and Mick Thomure were supported under a summer students program at Fermilab.

REFERENCES

[1] Xinhua, Bai, "Test of the Aging Effect of a Bag Liner with a Small Water Cerenkov Detector," Pierre Auger Project Technical Note GAP-98-010 (1998).

[2] Filipcic, A., "The Time Stability of a Small Water Cerenkov Detector," Pierre Auger Project Technical Note GAP-98-*** (1998).

[3] Strom, D., "Stability of Water in a Small Cerenkov Detector," Fermilab summer student report (1999). The uncertainties on the fitted peaks are too small by $2^{1/2}$ in this report because of an error in the EXCEL analysis. This error was located by the comparison of these data with the alternate analysis results.

[4] Ravignani, D., P. Bauleo, A. Etchegoyen, A.M.J. Ferrero, A. Filevich, C.K. Guerard, F. Hasenbalg, and J. Rodriguez Martino, "Calculation of the Number of Photoelectrons with the Water Cerenkov Detector Model," Pierre Auger Project Technical Note GAP-97-024 (1997).

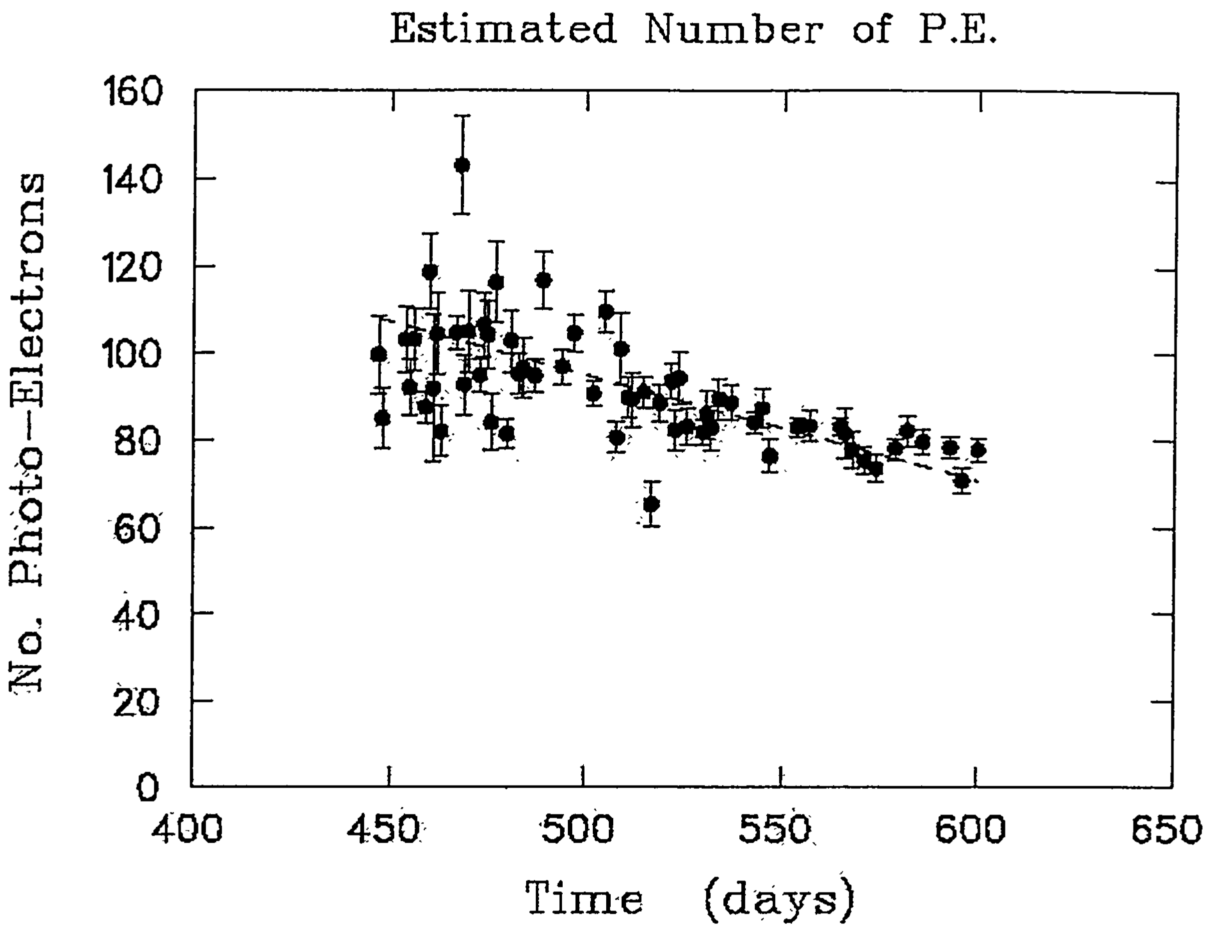

Figure 8. Variation of the derived number of photoelectrons as a function of time for the June, 1999 to November, 1999 runs. The errors include the contribution from the pedestal uncertainty. The dashed curve shows the approximate expected behavior from the straight line fit to the data in Fig. 7.

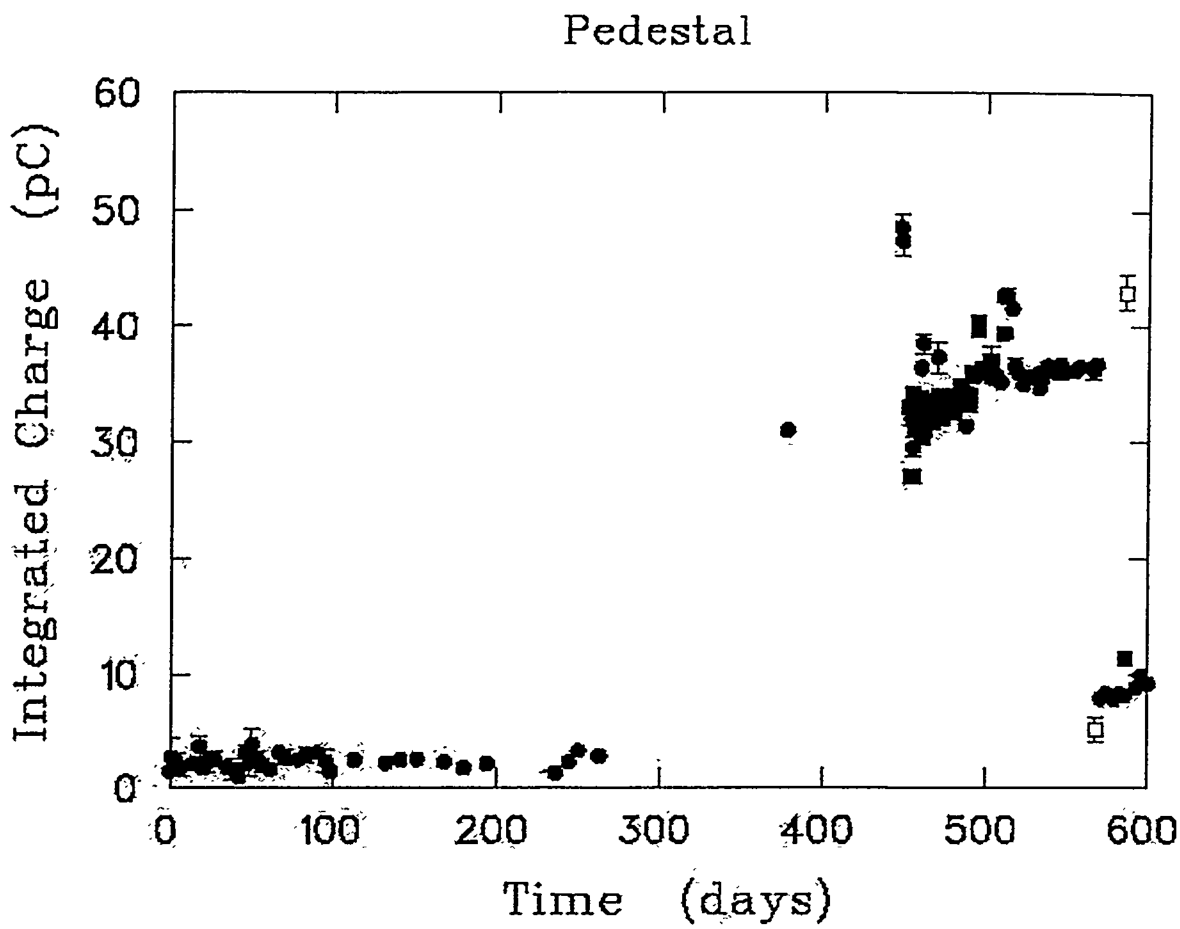

Figure 9. Variation of the pedestal in the ADC spectra as a function of time for the runs from March, 1998 until November, 1999. The solid squares are from dedicated pedestal runs and the solid circles from normal cosmic ray runs.

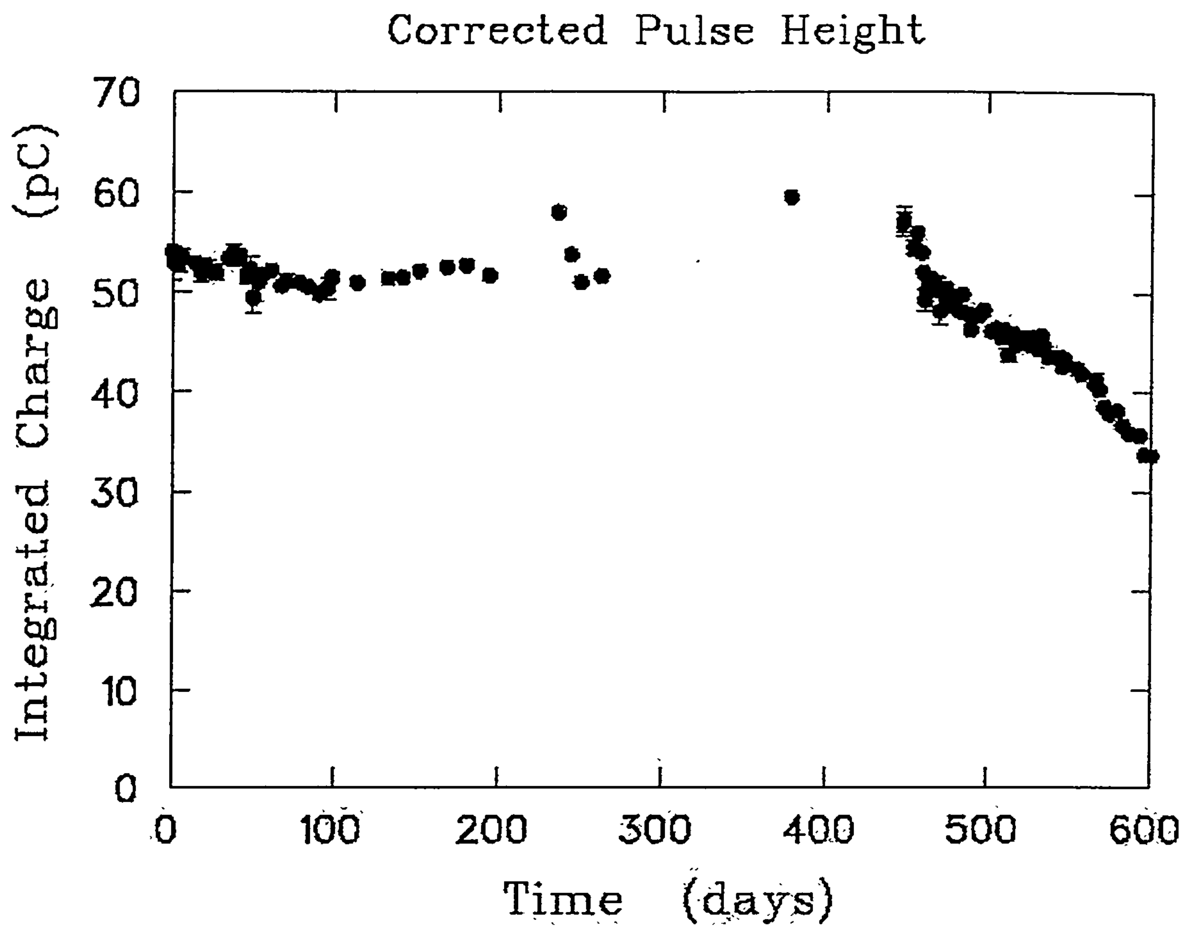

Figure 10. Plot of the peak positions corrected for pedestals for the March, 1998 to November, 1999 runs.

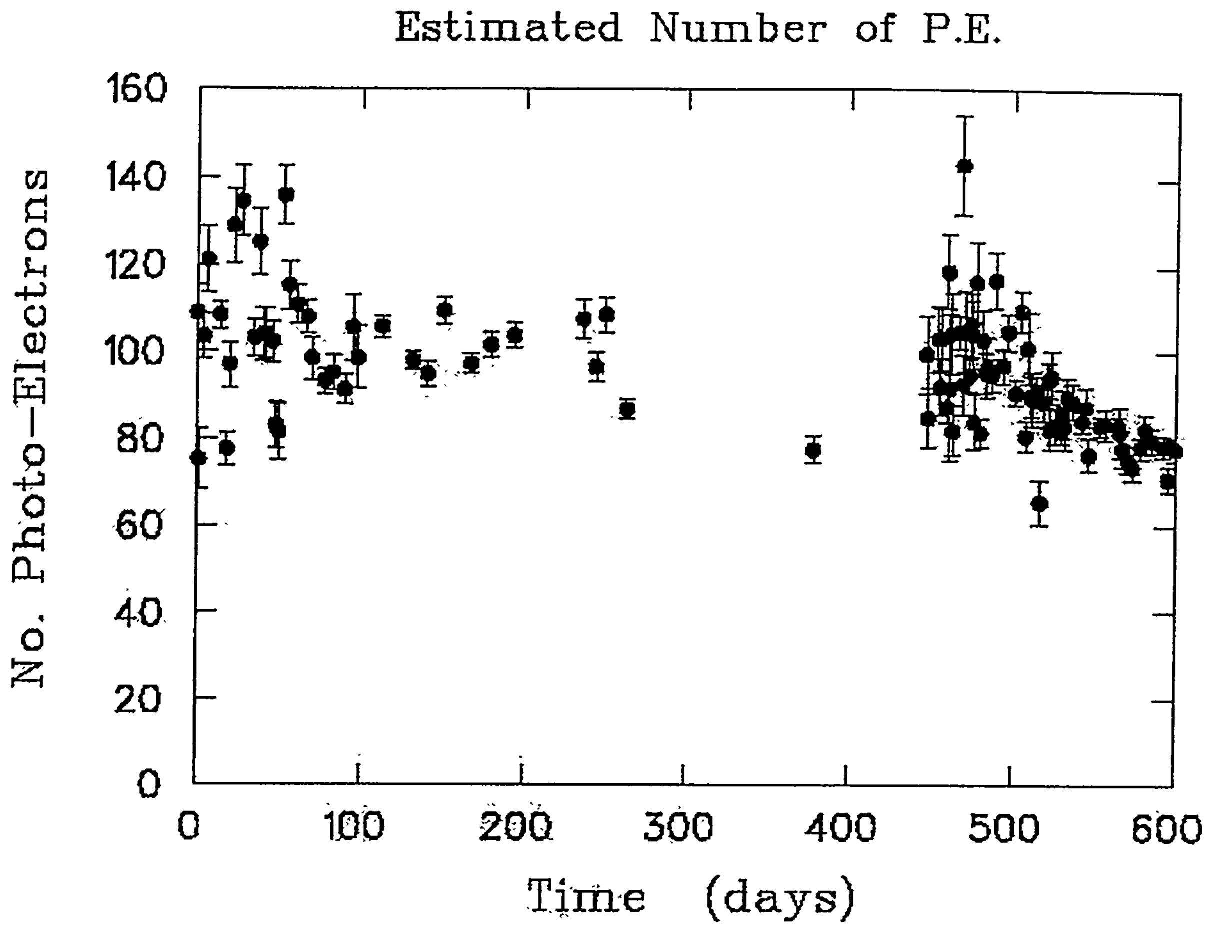

Figure 11. Plot of the computed number of photoelectrons as a function of time for the June to November, 1999 runs. The errors include the contribution from the pedestal uncertainty.

Table 1.

Pedestals for data runs with the small tank between March, 1998 and November, 1999. The date quoted is the day the run ended. The error is the uncertainty on the mean pedestal. The number of events in the pedestal region is also shown. The pedestal and error are in units of pC.

Run Number	*Date*	*Day*	*Pedestal*	*Error*	*Events*
tst1942	03/26/98	0	1.45	0.42	10
tst1943	03/27/98	1	2.64	1.66	6
tst1944	03/30/98	4	2.32	0.73	20
tst1945	04/01/98	6	1.67	0.70	15
tst1946	04/09/98	14	2.11	0.37	58
tst1947	04/13/98	18	3.62	0.88	15
tst1948	04/15/98	20	1.72	0.59	15
tst1949	04/17/98	22	2.21	0.87	11
tst1952	04/22/98	27	2.53	0.72	18
tst1954	04/30/98	35	1.78	0.59	17
tst1956	05/03/98	38	1.64	0.89	11
tst1957	05/05/98	40	1.41	0.67	8
tst1958	05/07/98	42	0.90	0.60	10
tst1959	05/11/98	46	2.99	0.75	22
tst1960	05/13/98	48	2.14	1.12	9
tst1961	05/15/98	50	3.78	1.46	7
tst1962	05/18/98	53	2.55	0.66	24
tst1963	05/21/98	56	1.93	0.61	18
tst1964	05/26/98	61	1.64	0.51	33
tst1965	06/01/98	67	3.06	0.50	51
tst1966	06/04/98	70	2.66	0.72	19
tst1967	06/12/98	78	2.53	0.41	56
tst1968	06/17/98	83	2.82	0.65	29
tst1969	06/24/98	90	3.07	0.55	42
tst1970	06/29/98	95	2.34	1.03	11
tst1972	07/02/98	98	1.45	0.40	60
tst1973	07/17/98	113	2.44	0.31	90
tst1975	08/05/98	132	2.19	0.31	102
tst1976	08/14/98	141	2.45	0.39	67
tst1977	08/24/98	151	2.53	0.40	65
tst1978	09/10/98	168	2.27	0.31	106
tst1979	09/22/98	180	1.75	0.37	56
tst1980	10/06/98	194	2.09	0.41	59
tst1984	11/17/98	236	1.30	0.47	21
tst1985	11/25/98	244	2.22	0.48	39
tst1986	12/01/98	250	3.21	0.47	35
tst1987	12/14/98	263	2.77	0.40	61
	The tank was moved after this run.				
tst1991	06/16/99	447	48.46	1.17	13
tst1993	06/17/99	448	47.36	1.24	11

Run Number	Date	Day	Pedestal	Error	Events
tst2001	06/22/99	453	33.05	0.28	56
tst2002	06/23/99	454	32.11	0.67	15
tst2003	06/23/99	454	27.10	0.11	29
tst2004	06/24/99	455	29.63	0.79	15
tst2005	06/24/99	455	34.27	0.38	31
tst2006	06/25/99	456	31.28	0.41	10
tst2007	06/25/99	456	31.29	0.18	56
tst2008	06/28/99	459	31.51	0.35	43
tst2009	06/28/99	459	30.63	0.12	40
tst2010	06/29/99	460	36.54	0.57	25
tst2011	06/29/99	460	33.99	0.044	142
tst2013	06/30/99	461	38.59	0.85	11
tst2014	06/30/99	461	30.38	0.17	53
tst2015	07/01/99	462	32.83	1.02	12
tst2016	07/01/99	462	31.09	0.079	55
tst2017	07/02/99	463	33.18	0.67	20
tst2018	07/02/99	463	31.71	0.072	63
tst2019	07/06/99	467	32.22	0.43	45
tst2020	07/06/99	467	31.85	0.065	65
tst2021	07/07/99	468	32.67	0.87	16
tst2022	07/07/99	468	32.47	0.064	74
tst2024	07/08/99	469	33.46	0.73	18
tst2025	07/08/99	469	33.47	0.14	60
tst2026	07/09/99	470	37.44	1.32	8
tst2027	07/09/99	470	34.12	0.056	79
tst2028	07/12/99	473	32.05	0.38	61
tst2029	07/12/99	473	32.99	0.075	120
tst2030	07/13/99	474	33.87	0.43	19
tst2031	07/13/99	474	33.06	0.13	190
tst2032	07/14/99	475	33.43	0.71	14
tst2033	07/14/99	475	33.49	0.081	187
tst2034	07/15/99	476	33.77	0.85	16
tst2035	07/15/99	476	32.92	0.052	124
tst2036	07/16/99	477	32.93	0.90	11
tst2038	07/19/99	480	33.84	0.32	52
tst2039	07/19/99	480	32.82	0.28	60
tst2040	07/20/99	481	34.13	0.12	121
tst2041	07/22/99	483	34.24	0.48	40
tst2042	07/22/99	483	34.87	0.012	2000
tst2043	07/22/99	483	34.83	0.006	6001
tst2044	07/22/99	483	34.79	0.006	6501
tst2045	07/22/99	483	34.79	0.006	7501
tst2046	07/23/99	484	34.12	0.54	15
tst2047	07/23/99	484	34.83	0.006	6001
tst2048	07/23/99	484	34.00	0.040	217
tst2049	07/26/99	487	31.47	0.34	59
tst2050	07/26/99	487	34.34	0.006	9213
tst2051	07/26/99	487	34.24	0.011	2156
tst2052	07/28/99	489	33.28	0.61	36
tst2053	07/28/99	489	34.09	0.016	1001
tst2054	07/28/99	489	34.04	0.016	1000

Run Number	Date	Day	Pedestal	Error	Events
tst2056	07/30/99	491	36.03	0.008	7701
tst2057	07/30/99	491	35.76	0.068	66
tst2058	08/02/99	494	35.94	0.26	73
tst2059	08/02/99	494	40.52	0.024	1001
tst2060	08/02/99	494	39.78	0.20	63
tst2061	08/05/99	497	36.32	0.31	26
tst2062	08/05/99	497	36.38	0.005	10000
tst2063	08/10/99	502	35.68	0.30	87
tst2064	08/10/99	502	37.17	1.20	3
tst2065	08/13/99	505	35.87	0.37	44
tst2066	08/16/99	508	35.29	0.54	34
tst2068	08/17/99	509	42.72	0.53	10
tst2069	08/17/99	509	39.48	0.010	2425
tst2071	08/19/99	511	39.50	0.53	31
tst2072	08/20/99	512	42.66	0.68	19
tst2073	08/23/99	515	41.65	0.32	42
tst2075	08/25/99	517	36.65	0.65	18
tst2076	08/27/99	519	36.10	0.42	41
tst2077	08/30/99	522	35.07	0.35	55
tst2078	08/31/99	523	35.68	0.57	25
tst2079	09/01/99	524	35.46	0.50	23
tst2080	09/03/99	526	35.81	0.57	27
tst2081	09/07/99	530	35.60	0.30	68
tst2082	09/08/99	531	36.01	0.58	21
tst2083	09/09/99	532	34.75	0.31	23
tst2084	09/11/99	534	35.68	0.54	20
tst2085	09/14/99	537	36.70	0.44	53
tst2086	09/20/99	543	36.09	0.29	99
tst2087	09/22/99	545	36.86	0.52	40
tst2088	09/24/99	547	36.13	0.45	39
tst2089	10/01/99	554	36.30	0.26	118
tst2090	10/04/99	557	36.60	0.45	47
tst2091	10/12/99	565	36.46	0.26	130
tst2092	10/13/99	566	36.31	0.75	17
tst2093	10/15/99	568	36.83	0.59	27
tst2094	10/15/99	568	5.15	1.07	5
tst2095	10/18/99	571	7.88	0.36	63
tst2096	10/21/99	574	8.29	0.48	58
tst2097	10/26/99	579	7.82	0.25	109
tst2098	10/29/99	582	8.27	0.37	65
tst2099	11/02/99	586	8.16	0.33	79
tst2100	11/02/99	586	43.00	1.49	4
tst2101	11/02/99	586	59.32	0.072	100
tst2102	11/02/99	586	11.29	0.056	101
tst2103	11/09/99	593	8.80	0.28	129
tst2104	11/12/99	596	9.85	0.40	78
tst2105	11/16/99	600	9.21	0.29	84

Table 2.

Peak positions for data runs with the small tank between March, 1998 and November, 1999. The raw peak position and its uncertainty (Peak, Error), the peak width (Sigma), and the number of events in the fitted peak (N) are shown for both the EXCEL analysis and (for some runs) the alternate analysis. In the latter case, the true number of events is shown as Events. The peak, error, and sigma values are all in units of pC.

		EXCEL Analysis				**Alternate Analysis**			
Run Number	*Day*	*Peak*	*Error*	*Sigma*	*N*	*Peak*	*Error*	*Sigma*	*Events*
tst1942	0	55.559	0.180	6.35	1246				
tst1943	1	55.545	0.247	7.47	910				
tst1944	4	55.116	0.132	6.36	2316				
tst1945	6	55.298	0.147	5.97	1243				
tst1946	14	55.053	0.079	6.23	6202				
tst1947	18	55.488	0.123	7.21	3416				
tst1948	20	54.459	0.157	6.56	1751				
tst1949	22	54.571	0.161	5.65	1228				
tst1952	27	54.508	0.146	5.49	1412				
tst1954	35	55.168	0.112	6.44	3286				
tst1956	38	55.522	0.150	5.90	1543				
tst1957	40	54.654	0.165	6.40	1488				
tst1958	42	54.619	0.165	6.45	1520				
tst1959	46	54.517	0.112	6.24	3150				
tst1960	48	54.490	0.170	7.03	1704				
tst1961	50	53.192	0.175	6.70	1456				
tst1962	53	53.553	0.115	5.36	2204				
tst1963	56	53.725	0.127	5.91	2162				
tst1964	61	53.812	0.099	6.07	3774				
tst1965	67	53.714	0.089	5.97	4529				
tst1966	70	53.776	0.130	6.31	2372				
tst1967	78	53.539	0.082	6.47	6313				
tst1968	83	53.404	0.100	6.35	4019				
tst1969	90	52.925	0.088	6.39	5308				
tst1970	95	52.750	0.180	6.01	1122				
tst1972	98	52.934	0.223	6.35	803				
tst1973	113	53.408	0.058	6.07	11176				
tst1975	132	53.613	0.052	6.36	14942				
tst1976	141	53.945	0.078	6.47	6901				
tst1977	151	54.727	0.071	6.11	7402				
tst1978	168	54.798	0.058	6.52	12666				
tst1979	180	54.530	0.072	6.41	7821				
tst1980	194	53.854	0.065	6.22	9064				
tst1984	236	59.341	0.133	6.85	2636				
tst1985	244	56.026	0.092	6.70	5290				
tst1986	250	54.278	0.093	6.00	4086				
tst1987	263	54.491	0.072	6.79	8718				

The tank was moved after this run.

		EXCEL Analysis				Alternate Analysis			
Run Number	*Day*	*Peak*	*Error*	*Sigma*	*N*	*Peak*	*Error*	*Sigma*	*Events*
tst1991	447	105.383	0.273	6.98					
tst1993	448	104.675	0.263	7.61					
tst2002	454	86.784	0.222	6.59					
tst2004	455	84.183	0.219	6.96					
tst2006	456	87.320	0.228	6.75					
tst2008	459	85.644	0.133	7.08	2830	85.269	0.143	7.75	2936
tst2010	460	88.695	0.195	5.86					
tst2013	461	87.927	0.564	6.30					
tst2015	462	83.180	0.245	6.03					
tst2017	463	84.662	0.228	6.96					
tst2019	467	83.474	0.103	6.13	3564	82.686	0.117	7.28	3905
tst2021	468	83.537	0.185	5.21					
tst2024	469	84.217	0.221	6.45					
tst2026	470	85.726	0.197	5.77					
tst2028	473	82.211	0.119	6.30	2848	81.311	0.130	7.13	3024
tst2030	474	84.481	0.199	6.00					
tst2032	475	82.901	0.205	5.93					
tst2034	476	83.414	0.225	6.63					
tst2036	477	81.981	0.194	5.57					
tst2038	480	83.466	0.126	6.73	2872	82.302	0.132	7.17	2951
tst2040	481	82.677	0.199	5.86	858	81.692	0.229	7.17	976
tst2041	483	82.489	0.140	6.05	1854	81.468	0.152	6.75	1960
tst2046	484	84.069	0.212	6.22					
tst2049	487	79.533	0.115	6.04	2778	78.905	0.126	6.86	2952
tst2052	489	79.708	0.126	5.26					
tst2058	494	83.731	0.115	5.94	2670	83.094	0.128	6.92	2897
tst2061	497	84.737	0.110	5.79					
tst2063	502	81.977	0.088	5.95	4546	81.105	0.095	6.59	4802
tst2065	505	82.416	0.106	5.44	2660	81.871	0.122	6.69	3016
tst2066	508	80.870	0.116	6.21					
tst2068	509	89.213	0.214	5.66					
tst2071	511	85.604	0.130	5.95					
tst2072	512	86.539	0.175	5.68					
tst2073	515	87.746	0.112	5.91	2782	86.494	0.120	6.51	2916
tst2075	517	81.555	0.238	6.80					
tst2076	519	81.114	0.130	5.85	2032	79.585	0.136	6.22	2080
tst2077	522	80.780	0.110	5.78	2768	79.682	0.120	6.45	2874
tst2078	523	80.778	0.161	6.08					
tst2079	524	81.119	0.177	5.75					
tst2080	526	80.673	0.133	6.02					
tst2081	530	80.198	0.102	6.03	3478	78.767	0.106	6.29	3537
tst2082	531	80.484	0.175	5.87	1112				
tst2083	532	80.581	0.180	6.16	1166				
tst2084	534	80.384	0.130	5.78	1960				
tst2085	537	80.339	0.110	5.67	2641	79.017	0.118	6.12	2712
tst2086	543	79.893	0.076	5.84	5927	78.368	0.079	6.13	6034
tst2087	545	79.579	0.122	5.59	2096	78.220	0.131	6.10	2164
tst2088	547	79.548	0.139	6.08	1938	77.987	0.142	6.30	1960
tst2089	554	78.824	0.068	5.71	7146	77.418	0.071	6.07	7311
tst2090	557	78.551	0.106	5.62	2828	77.090	0.110	5.88	2879

		EXCEL Analysis				Alternate Analysis			
Run Number	*Day*	*Peak*	*Error*	*Sigma*	*N*	*Peak*	*Error*	*Sigma*	*Events*
tst2091	565	77.370	0.062	5.49	7841	75.857	0.065	5.81	8009
tst2092	566	77.514	0.165	5.58	1129				
tst2093	568	77.209	0.137	5.60	1946				
tst2094	568	48.811	0.327	5.67	300				
tst2095	571	46.476	0.105	5.44	2736	44.812	0.107	5.61	2773
tst2096	574	46.196	0.095	5.41	3231	44.540	0.096	5.46	3256
tst2097	579	46.027	0.075	5.29	5045	44.457	0.076	5.46	5108
tst2098	582	45.026	0.095	4.96	2774	43.546	0.100	5.31	2842
tst2099	586	44.110	0.078	4.93	4003	42.400	0.080	5.11	4063
tst2100	586	80.205	0.412	5.14	156				
tst2103	593	44.464	0.061	4.93	6558	42.924	0.064	5.25	6710
tst2104	596	43.537	0.090	4.90	3084				
tst2105	600	42.848	0.072	4.67	4188				